FMNL2 regulates actin for ER and mitochondria distribution in oocyte meiosis

Meng-Hao Pan[1, 2], Zhen-Nan Pan[1], Ming-Hong Sun[1], Xiao-Han Li[1], Jia-Qian Ju[1], Shi-Ming Luo[2], Xiang-Hong Ou[2], Shao-Chen Sun[1*]

[1]College of Animal Science and Technology, Nanjing Agricultural University, Nanjing 210095, China.

[2]Fertility Preservation Lab, Reproductive Medicine Center, Guangdong Second Provincial General Hospital, Guangzhou, China.

Running Title: FMNL2 in mouse oocytes

[*]**Correspondence to:** Shao-Chen Sun, College of Animal Science and Technology, Nanjing Agricultural University, Nanjing 210095, China. E-mail: sunsc@njau.edu.cn

Funding: This work was supported by the National Natural Science Foundation of China (32170857); the National Key Research and Development Program of China (2021YFC2700100).

There is no conflict of interest to declare.

Abbreviations: FMNL2, Formin-like 2; FMNLs, Formin-likes; GV, germinal vesicle; GVBD, germinal vesicle breakdown; ATI, anaphase-telophase I; MI, metaphase I; MII, metaphase II; ER, Endoplasmic reticulum.

Abstract

During mammalian oocyte meiosis, spindle migration and asymmetric cytokinesis are unique steps for the successful polar body extrusion. The asymmetry defects of oocytes will lead to the failure of fertilization and embryo implantation. In present study we reported that an actin nucleating factor formin-like 2 (FMNL2) played critical roles in the regulation of spindle migration and organelle distribution. Our results showed that FMNL2 mainly localized at the oocyte cortex and periphery of spindle. Depletion of FMNL2 led to the failure of polar body extrusion and large polar bodies in oocytes. Live-cell imaging revealed that the spindle failed to migrate to the oocyte cortex, which caused polar body formation defects, and this might be due to the decreased polymerization of cytoplasmic actin by FMNL2 depletion. Furthermore, mass spectrometry analysis indicated that FMNL2 was associated with mitochondria and endoplasmic reticulum-related proteins, and FMNL2 depletion disrupted the function and distribution of mitochondria and endoplasmic reticulum, showing with decreased mitochondrial membrane potential and the occurrence of endoplasmic reticulum stress. Microinjecting Fmnl2-EGFP mRNA into FMNL2-depleted oocytes significantly rescued these defects. Thus, our results indicate that FMNL2 is essential for the actin assembly, which further involves into meiotic spindle migration and ER/mitochondria functions in mouse oocytes.

Keywords: FMNL2; oocyte; actin; Endoplasmic reticulum; Mitochondria

Introduction

Mammalian oocyte maturation is an asymmetric division process that generates a large egg and a small polar body. This asymmetry is critical for the following fertilization and early embryo development. After germinal vesicle breakdown (GVBD), the meiotic spindle is organized at the center of the oocyte, and then it migrates to the oocyte cortex at the late metaphase I (MI). The oocytes are arrested at metaphase II (MII) after the extrusion of first polar body (*1, 2*). Actin filaments, as the most widely distributed cytoskeleton in cells, regulate various dynamic events during oocyte meiotic maturation (*3*), and two key events are the spindle migration and cortical reorganization in mammalian oocytes (*1, 4, 5*). Small GTPases and actin nucleation factors are shown to promote the assembly and function of actin. The actin nucleation factors are the molecules that directly promote the actin assembly: Arp2/3 complex control the assembly of branched actin, and formin family member Formin2 (FMN2) and Spire1/2 control the assembly of linear actin. These proteins are all proposed to play a role in actin-related spindle migration and cytokinesis during mammalian oocyte maturation (*6-8*). The cortex protein Arp2/3 complex nucleates the actin to produce a hydrodynamic force to move the spindle toward the cortex, and regulates cytokinesis during oocyte maturation (*1, 8*). FMN2 and Spire1/2 nucleates actin around the spindle in the cytoplasm to give the meiotic spindle an initial power for migration (*7, 9*).

Besides Formin2, the DRFs (diaphanous-related formins) subfamily in the formin family has been extensively studied. The DRFs family consists of mDia, Daam, FHOD and FMNLs (*10*). The “Formin-like” proteins (FMNLs) subfamily includes FMNL1

(FRL1), FMNL2 (FRL3), and FMNL3 (FRL2). Like other Formin family proteins, FMNLs play important roles in cell migration, cell division, and cell polarity (*10, 11*). While FMNL2 is widely expressed in multiple human tissues, especially in the gastrointestinal and mammary epithelia, lymphatic tissues, placenta, and reproductive tract (*12*). As an important actin assembly factor, FMNL2 accelerates the elongation of actin filaments branched by Arp2/3 complex (*13*). In invasive cells, FMNL2 is mainly localized in the leading edge of the cell, lamellipodia and filopodia tips, to improve cell migration ability by actin-based manner (*13-15*). FMNL2 is also involved in the maintenance of epithelial-mesenchymal transition (EMT) in human colorectal carcinoma cell (*16*). Besides its roles on the actin assembly, emerging evidences indicate that FMNL2 may interact with organelle dynamics. It is shown that FMNL2 is related with the Golgi apparatus, since the absence of FMNL2/3 can cause the Golgi fragmentation (*17*). However, till now the roles of FMNLs especially FMNL2 on oocyte meiosis are still largely unknown.

In the present study, we disturbed the FMNL2 expression and explored the roles of FMNL2 during mouse oocyte meiosis. Our results showed that FMNL2 was essential for the polar body size control and successful extrusion; and these abnormal phenotypes might be due to aberrant actin-based meiotic spindle migration. Meanwhile, we also found that FMNL2 was essential for the functions and distribution of mitochondria and endoplasmic reticulum. Therefore, this study provided the evidence for the critical roles of FMNL2-mediated actin on spindle movement and organelle dynamics in mammalian oocytes.

Materials and Methods

Antibodies and chemicals

Rabbit monoclonal anti-FMNL2 antibody, rabbit monoclonal anti-Arp2 antibody, mouse monoclonal anti-profilin1 antibody were from Santa Cruz (Santa Cruz, CA, USA). Rabbit monoclonal anti-Fascin antibody was purchased form Abcam (Cambridge, UK). Rabbit polyclonal anti-INF2 antibody was purchased from Proteintech (Proteintech, CHI, USA). Rabbit monoclonal anti-α-tubulin (11H10) antibody, rabbit monoclonal anti-Grp78 antibody, rabbit monoclonal anti-cofilin antibody and rabbit monoclonal anti-Chop antibody were from Cell Signaling Technology (Beverly, MA, USA). Mouse monoclonal anti-α-tubulin-FITC antibody was from Sigma-Aldrich Corp. (St. Louis, MO, USA). FITC-conjugated goat anti-rabbit IgG were from Zhongshan Golden Bridge Biotechnology (Beijing). ER-Tracker Red and Mito-Tracker Green were from Beyotime Biotechnology (Shanghai). All other chemicals and reagents were from Sigma-Aldrich Corp., unless otherwise stated.

Ethics statement and oocyte culture

We followed the guidelines of Animal Research Institute Committee of Nanjing Agricultural University to conduct the operations. The animal facility had license authorized by the experimental animal committee of Jiangsu Province (SYXK-Su-20170007). These mice were housed in considerably ideal conditions which consisted of controlled temperature, regular diet and appropriate light. Female mice (4 - 6 weeks) were used to collect germinal vesicle oocytes. The oocytes were placed at 37°C with an atmosphere of 5% CO2, and cultured to different time points for immunostaining,

111 microinjection and western blot.

Plasmid construct and in *vitro* transcription

112 Template RNA was generated from mouse ovaries with RNA Isolation Kit
113 (Thermos fisher), then we reversed transcription of these RNA to create cDNA by a
114 PrimeScript 1st strand cDNA synthesis kit (Takara, Japan). Fmnl2-EGFP vector was
115 generated by Wuhan GeneCreate Biological Engineering Co, Ltd. mRNA was
116 synthesized from linearized plasmid using HiScribe T7 high yield RNA synthesis kit
117 (NEB), then capped with m7G(5')ppp(5')G (NEB) and tailed with a poly(A)
118 polymerase tailing kit (Epicentre) and purified with RNA clean & concentrator-25 kit
119 (Zymo Research).

Microinjection of Fmnl2 siRNA and mRNA

120 Fmnl2 siRNA microinjection was used to knock down endogenous Fmnl2 in
121 mouse oocytes. Fmnl2 siRNA 5′- GCU GAA UGC UAU GAA CCU ATT-3′, 5′- GCC
122 AUU GAU CUU UCU UCA ATT-3′, 5′- GGA AUU AAG AAG GCG ACA ATT-3′,
123 (Genepharma, Shanghai, China) were diluted with DEPC water to give a 20μM stock
124 solution respectively, and the three siRNA were mixed in equal proportions before
125 microinjection. The control group was microinjected with negative control siRNA 5′-
126 UUC UCC GAA CGU GUC ACG UTT-3′. After injection, the oocytes were cultured
127 in M16 medium containing 5μM milrinone for 18-20 h, and then washed five times (2
128 min each) in fresh M2 medium. We transferred the oocytes to fresh M16 medium, and
129 cultured for following experiments. When microinjecting the α-tubulin-EGFP mRNA
130 and rescue experiments, GV oocytes need to be cultured in M16 medium with 5μM

131 milrinone for 2h. DNase/RNase-free water microinjected as the control.

Immunofluorescent staining and confocal microscopy

132 Oocytes were fixed in 4% paraformaldehyde (in PBS) for 30 min and
133 permeabilized with 0.5% Triton X-100 in PBS for 20min then blocked in blocking
134 buffer (1% BSA-supplemented PBS) at room for 1 h. For FMNL2 staining, the oocytes
135 after blocking were incubated with Rabbit monoclonal anti-FMNL2 antibody (1:100)
136 at 4 °C overnight, then oocytes were washed by wash buffer (0.1% Tween 20 and 0.01%
137 Triton X-100 in PBS) for 3 times (5 min each time). Next the oocytes were labeled with
138 secondary antibody coupled to FITC-conjugated goat anti-rabbit IgG (1:100) at room
139 temperature for 1 h. For α-tubulin staining, oocytes were incubated with anti-α-tubulin-
140 FITC antibody (1:200). For actin staining, oocytes were incubated with Phalloidin-
141 TRITC at room temperature for 2 h. Then the oocytes were washed as the same way.
142 Finally, oocytes were incubated with Hoechst 33342 at room temperature for 10-20 min.
143 After staining, samples were mounted on glass slides and observed with a confocal
144 laser-scanning microscope (Zeiss LSM 800 META, Germany).

ER and Mito-tracker staining

145 To study ER and mitochondria distribution during mouse oocyte meiosis, MI stage
146 oocytes were incubated with ER-Tracker Red (1:3000) or 200 nM Mito-tracker green
147 (Red) in M16 medium for 30 min at 37ºC and 5% CO2. Then the oocytes were washed
148 three times with M2 medium, finally the samples were examined with confocal
149 microscopy.

Time lapse microscopy

To image the dynamic changes that occurred during oocyte maturation, oocytes were cultured in M16 medium, then transferred to the Leica SD AF confocal imaging system equipped with 37 °C incubator and 5% CO2 supply (H301-K-FRAME). The spindle in oocytes was labeled by α-tubulin-EGFP.

Immunoprecipitation

4-6 ovaries were put into RIPA Lysis Buffer contained phosphatase inhibitor cocktail (100×) (Kangwei Biotechnology, China), and were completely cleaved on ice block. We collected supernatant after centrifugation (13200 rps, 20 min) and then took out 50 μl as input sample at 4 °C. The rest of the supernatant was incubated with primary antibody (FMNL2 or INF2 antibody) overnight at 4 °C. 30 μl conjugated beads (washed five times in PBS) were added to the supernatant/antibody mixture and incubated at 4 °C for 4-6 h, after three times wash by immune complexes, the samples were then released from the beads by mixing in 2× SDS loading buffer for 10min at 30 °C.

Western blot analysis

Approximate 100-150 mouse oocytes were placed in Laemmli sample buffer and heated at 85℃ for 7-10 min. Proteins were separated by SDS-PAGE at 165V for 70-80 min and then electrophoretically transferred to polyvinylidene fluoride (PVDF) membranes (Millipore, Billerica, MA, USA) at 20 V for 1 hour. After transfer, the membranes were then blocked with TBST (TBS containing 0.1% Tween 20) containing 5% non-fat milk at room temperature for 90 min. After blocking, the membranes were incubated with rabbit monoclonal anti-FMNL2 antibody (1:500), rabbit monoclonal anti-Arp2 antibody (1:500), mouse monoclonal anti-profilin1 antibody (1:500), rabbit

monoclonal anti-Fascin antibody (1:5000), rabbit polyclonal anti-INF2 antibody (1:500), rabbit monoclonal anti-Grp78 antibody (1:1000), rabbit monoclonal anti-cofilin antibody (1:2000), rabbit monoclonal anti-CHOP antibody (1:1000), or rabbit monoclonal anti-tubulin antibody (1:2000) at 4 °C overnight. After washing 5 times in TBST (5 min each), membranes were incubated for 1h at room temperature with HRP-conjugated Pierce Goat anti-Rabbit IgG (1:5000) or HRP-conjugated Pierce Goat anti-mouse IgG (1:5000). After washing for 5 times, the membranes were visualized using chemiluminescence reagent (Millipore, Billerica, MA). Every experiment repeated at least 3 times with different samples.

Intensity analysis

To analyze the fluorescence intensity of actin filaments, the control group and treated group were mounted on the same glass slide and tested with same parameters. Image J was used to determine the average fluorescence intensity per unit area within the region of interest (ROI). The independent measures were taken for the cell cortex and cytoplasm. For quantification of the western blot results, the band intensity was measured by Image J.

Statistical analysis

At least three biological replicates were performed for each analysis. The results were endowed as means ± SEM. All analyses were performed using GraphPad Prism7.00 software (GraphPad, CA, USA). Results of $P<0.05$ were considered statistically significant (differences $P<0.05$ denoted by *, $P<0.01$ denoted by **, $P<0.001$ denoted by *** and $P<0.0001$ denoted by ****).

Results

Expression and subcellular localization of FMNL2 during mouse oocyte maturation

We first examined FMNL2 expression in mouse oocytes at different stages. The results indicated that FMNL2 all expressed in GV, MI and MII stages during mouse oocyte maturation (GV, 1; MI, 0.82 ± 0.07; MII, 0.61 ± 0.10, Figure 1A). Next, we performed Fmnl2-EGFP mRNA microinjection to examine the localization of FMNL2. As shown in Figure 1B, FMNL2 accumulated at the oocyte cortex during the GV, GVBD and MI stages. Besides, FMNL2 also localized at the spindle periphery during GVBD and MI stages. At anaphase-telophase I stage (ATI), FMNL2 was mainly at the midbody. The FMNL2 antibody staining results also confirmed this localization pattern. We also co-stained FMNL2 antibody with actin, and the result showed that the signals of FMNL2 and actin overlapped at the cortex in oocytes (Figure 1C). The FMNL2 localization pattern indicated that FMNL2 might interact with actin dynamics during oocyte meiosis.

FMNL2 is essential for polar body extrusion and asymmetric division in mouse oocytes

To investigate the functional roles of FMNL2 in mouse oocytes, we employed Fmnl2 siRNA microinjection to knockdown FMNL2 protein expression. A significant decrease of FMNL2 protein level was shown in FMNL2-KD oocytes compared to control group by western blot (1 vs. 0.48 ± 0.08, $P < 0.01$, Figure 2A). We then examined first polar body extrusion, and the results showed that deleting FMNL2

207 disturbed first polar body extrusion, while a large proportion of oocytes showed big
208 polar bodies among the oocytes which extruded polar bodies (Figure 2B). The
209 quantitative results also confirmed this phenotype (rate of polar body extrusion: 74.26
210 ± 1.44%, n = 439 vs. 59.5 ± 2.82%, n = 398, $P < 0.001$, Figure 2C; rate of large polar
211 bodies: 19.05 ± 1.97%, n = 311 vs. 37.16 ± 1.87%, n = 257, $P < 0.0001$, Figure 2D). In
212 addition, live-cell imaging was used to determine the dynamic changes that occurred
213 during oocyte maturation, and the results showed that the oocytes either failed to
214 undergo cytokinesis or divided from the central axis of the oocytes and formed big polar
215 bodies (Figure 2E). To further confirm the phenotype, we performed FMNL2 rescue
216 experiments by expressing exogenous Fmnl2 mRNA in FMNL2-depleted oocytes
217 (Figure 2F), we found that exogenous Fmnl2 mRNA expression rescued first polar body
218 extrusion and large polar body defects (Figure 2G). The quantitative results also
219 confirmed this phenotype (rate of polar body extrusion: 48.34 ± 4.2%, n = 355 vs. 62.62
220 ± 3.6%, n = 377, $P < 0.01$, Figure 2H; rate of large polar bodies: 30.93 ± 2%, n = 193
221 vs. 9.58 ± 2.4%, n = 203, $P < 0.01$, Figure 2I). To testify whether the functions of
222 FMNL2 were associated with other FMNLs, we also compared the polar body extrusion
223 with the knock down of both FMNL2 and FMNL3, and the results showed that double
224 knock down of FMNL2 and FMNL3 did not cause a severe polar body extrusion defects
225 compared with the single knock down of FMNL2 (polar body extrusion, Control: 70.97
226 ± 1.23%, n=261 vs FMNL2+3-KD: 60.42 ± 2.99%, n=198, $P < 0.05$, Figure 2J. Large
227 polar body, Control: 10.85 ± 0.97%, n=172 vs FMNL2+3-KD: 32.90 ± 1.88%, n=118,
228 $P < 0.001$, Figure 2K). These results suggested that FMNL2 played critical roles for the

polar body extrusion and asymmetric division during mouse oocyte maturation.

FMNL2 regulates spindle migration during mouse oocyte maturation

To investigate the causes for polar body extrusion defects, we examined the spindle migration by time-lapse microscopy during oocyte meiosis. As shown in Figure 4A, in the control oocyte, the meiotic spindle formed in the center of the oocyte after culture 8 h and moved to the oocyte cortex at 9.5h; and the polar body was extruded at 11-12h, with a spindle formed near the cortex at MII stage. However, in FMNL2-KD oocytes, two phenotypes were observed: 1) the meiotic spindle remained in the center of the oocyte until 10 h, and then the oocytes initiated the cytokinesis at 10.5 h but failed to extrude the polar body; 2) some oocytes with arrested spindles initiated the cytokinesis but extruded a big polar body (Figure 3A). This indicated the failure of spindle migration after FMNL2 depletion. We analyzed the rate of cortex-localized spindle in oocytes by cultured for 9.5 h, and the result showed that the rate of migrated spindles in control oocytes was significantly higher than that in FMNL2-KD oocytes (59.94 ± 3.42%, n = 78 vs. 38.97 ± 6.34%, n = 64, $P < 0.05$, Figure 3B). We also performed FMNL2 rescue experiments. Supplementing with exogenous Fmnl2 rescued the spindle migration defects compared with the Fmnl2-depletion group (40.27 ± 3.19%, n = 181 vs. 57.01± 2.72%, n = 57, $P < 0.01$, Figure 3C). These results suggested that FMNL2 might be involved in spindle migration in mouse oocytes.

FMNL2 promotes cytoplasmic actin assembly during mouse oocyte maturation

As FMNL2 is a key actin assembly factor, we further investigated actin assembly after deleting FMNL2 in mouse oocytes. Surprisingly there was no significant

difference for the signals of cortex actin was observed between control oocytes and FMNL2-KD oocytes, which was confirmed by the fluorescence intensity analysis (30.88 ± 1.10, n = 28 vs. 30.58 ± 1.12, n = 28, P > 0.05, Figure 4A). However, we found a significant decrease of cytoplasmic actin signals in the FMNL2-KD oocytes, and the statistical analysis for the cytoplasmic actin fluorescent signals also confirmed our findings (58.25 ± 2.05, n = 26 vs. 37.92 ± 2.02, n = 24, P < 0.0001, Figure 4B). Moreover, the rescue experiments showed that exogenous Fmnl2 rescued the decrease of cytoplasmic actin filaments compared with the Fmnl2-depletion group (37.98 ± 1.98, n = 16 vs. 54.72± 2.88, n = 15, P < 0.0001, Figure 3C). We next explored how FMNL2 regulates cytoplasmic actin assembly in oocytes. By mass spectrometry analysis we found there were several actin-related potential candidates which might be related with FMNL2 (Figure 4D). Co-immunoprecipitation results showed that FMNL2 precipitated Arp2 and Formin2 but not Profilin and fascin (Figure 4E). To further verify the correlation between FMNL2 and Arp2 and Formin2, we then examined Arp2 and Formin2 protein expression after FMNL2 knockdown. The results showed Arp2 protein expression increased significantly after FMNL2 knockdown (1 vs. 1.56 ± 0.07, P < 0.001, Figure 4F) but decreased after FMNL2 knockdown (1 vs. 0.62 ± 0.04, P < 0.001, Figure 4G). Exogenous Fmnl2 rescued these alterations compared with that in the FMNL2-KD group (Arp2 protein expression: 1 vs. 0.65 ± 0.06, P < 0.01, Figure 4F; Formin2 protein expression: 1 vs. 1.24 ± 0.05, P < 0.01, Figure 4G). These results indicated that FMNL2 associated with Formin2 and Arp2 for actin assembly in mouse oocytes.

FMNL2 regulates endoplasmic reticulum distribution during mouse oocyte maturation

The mass spectrometry analysis data indicated that several ER-related potential candidates which might be related with FMNL2 (Figure 5A), while INF2, a typical protein which mediates actin polymerization at ER showed high confidence level. We then examined the relationship between FMNL2 and INF2, and the co-immunoprecipitation results showed that FMNL2 precipitated INF2 and INF2 also precipitated FMNL2 (Figure 5B), indicating that FMNL2 interacted with INF2 in mouse oocytes. We then examined the ER distribution in FMNL2-KD oocytes. As shown in Figure 5C, in control oocytes the ER evenly distributed in the cytoplasm and accumulated at the spindle periphery in MI stage; however, ER agglomerated in cytoplasm in FMNL2-KD oocytes (Figure 5C). The statistical analysis showed that the abnormal distribution of ER increased significantly in the FMNL2-KD group (28.91 ± 5.62, n = 27 vs. 59.64 ± 6.95, n = 28, $P < 0.05$, Figure 5D). The localization pattern of ER indicated its functions might be disturbed. In FMNL2-KD oocytes, we found the expressions of ER-stress related proteins Grp78 and Chop were significantly increased (Grp78: 1 vs. 1.42 ± 0.12, $P < 0.05$; Chop: 1 vs. 1.53 ± 0.16, $P < 0.05$. Figure 5E), indicating the occurrence of ER stress. We also performed FMNL2 rescue experiments. Supplementing with exogenous Fmnl2 rescued the ER distribution defects caused by FMNL2 knockdown (Figure 5F), which was supported by the statistical analysis showing that the abnormal distribution rate of ER decreased significantly in the rescue group (52.04 ± 5.29, n = 70 vs. 34.91 ± 3.37, n = 78, $P < 0.05$, Figure 5G). Moreover,

Grp78 protein expression decreased in the rescue group (1 vs. 0.78 ± 0.05, $P < 0.01$. Figure 5H). These results indicated that the depletion of FMNL2 affected ER distribution and caused ER stress in mouse oocytes.

FMNL2 regulates mitochondrial distribution during mouse oocyte maturation

As INF2 is also related to the mitochondrial connection of ER, we further screened up the mass spectrometry analysis data and we found many mitochondria-related potential candidates which might be related with FMNL2 (Figure 6A). Therefore, we further examined the distribution of mitochondria in FMNL2-KD oocytes. In control oocytes, the mitochondria evenly distributed in the cytoplasm and accumulated at the spindle periphery in MI stage; however, in FMNL2-KD oocytes, mitochondria presented clumped aggregation distribution in cytoplasm (Figure 6B). We counted the number of clumps and found that the uniform distribution of mitochondria decreased significantly in the FMNL2-KD group (59.66 ± 8.48, $n = 31$ vs. 20.83 ± 4.17, $n = 32$, $P < 0.05$, Figure 6C). A large number of FMNL2-KD oocytes agglomerated into one to three clumps (22.73± 4.27, $n = 31$ vs. 42.50 ± 1.25, $n = 32$, $P < 0.05$, Figure 6C). Supplementing with exogenous Fmnl2 rescued the mitochondria distribution (Figure 6D), the statistical analysis showed that the uniform distribution of mitochondria increased significantly in the rescue group (36.49 ± 3.97, $n = 53$ vs. 53.90 ± 2.09, $n = 79$, $P < 0.05$, Figure 6E). We also examined mitochondrial membrane potential, and the results showed that FMNL2 depletion caused the alterations of mitochondrial membrane potential (MMP) by JC-1 staining. The fluorescence intensity of JC-1 red channel was decreased compared with the control group (Figure 6F). We also calculated

the ratio for red/green fluorescence intensity, and the results also confirmed this (control group: 0.40 vs. FMNL2-KD: 0.21 ± 0.01, $P < 0.01$) (Figure 6G). Cofilin is an important factor of actin assembly and regulates mitochondrial function. We also examined cofilin protein expression after FMNL2 knockdown. The results showed cofilin protein expression decreased significantly after FMNL2 knockdown (1 vs. 0.81 ± 0.03, $P < 0.01$, Figure 6H). These results indicated that FMNL2 regulated mitochondria distribution and function during mouse oocyte maturation.

Discussion

In this study, we explored the functions of FMNL2 during mouse oocyte meiosis. Our results indicated that FMNL2 regulated actin-based spindle migration for asymmetric cell division of oocytes, and more importantly FMNL2 was critical for maintaining the distribution of the ER and mitochondria, which set up a link for actin-related spindle migration and organelle dynamics in oocytes.

As a subfamily of Formin family, FMNLs play an important role in regulating actin filaments (*18*), while FMNL2 is most widely expressed in variety of cell models among the members of FMNLs. In this study, we showed that FMNL2 expressed in mouse oocytes and it mainly accumulated at the oocyte cortex and spindle periphery, which was similar with the actin distribution pattern in oocytes. This specific localization is also similar to FMN2, a well-studied factor in the formin family for spindle migration during oocyte meiosis (*7, 19*). In addition, another FMNLs family member, FMNL1 is also localized at the cortex and is essential for actin polymerization and spindle assembly during oocyte meiosis (*20*). Based on the localization pattern of FMNL2, we

speculated that the functions of FMNL2 might be also involved in actin-related process during mouse oocyte meiosis.

To confirm our hypothesis, we depleted FMNL2 protein expression and we found that absence of FMNL2 caused the aberrant first polar body extrusion. The oocytes either failed to form the polar body or extruded large polar bodies. These phenotypes caused by FMNL2 depletion are similar to the other actin-related proteins during oocyte maturation such as Arp2/3 complex (*8, 21*) and FMN2 (*22, 23*). We next examined the actin distribution in oocytes since it is reported that FMNL2 promotes actin filament assembly in many models. FMNL2 is required for cell-cell adhesion formation by regulating the actin assembly (*24*), and FMNL2 could directly drives actin elongation (*15*). In CRC cells, cortactin bind to FMNL2 to active the actin polymerization, and FMNL2 is important for invadopodia formation and functions (*25*). Our results showed that the FMNL2 depletion caused significantly decrease in cytoplasmic actin, indicating the conserved roles of FMNL2 on actin assembly in mammalian oocyte model. Other Formin family proteins such as Daam1, FHOD1, and Formin-homology family protein mDia1 are also reported to affect oocyte meiosis by regulating actin polymerization (*26-28*).

We then tried to explore how FMNL2 involves into the actin assembly in oocytes. Mass spectrometry analysis data indicated that FMNL2 associated with several actin-related proteins, and we found that FMNL2 was associated with Arp2 and Formin2. This could be confirmed by the altered expression of these two molecules after FMNL2 depletion. Therefore, we speculated FMNL2 could regulate cytoplasmic actin assembly

in oocytes through the association with Formin2 since it is reported to be an important protein for cytoplasmic actin assembly in oocytes (*22*). Interestingly, our results showed that unlike the reduction of cytoplasmic actin, cortex actin was not affected by the absence of FMNL2. We speculated that Arp2/3 complex has a compensation effect on the depleting of FMNL2 during oocyte meiosis, ensuring the cortex actin assembly in oocytes since Arp2 protein expression significantly increased after FMNL2 depletion. As an actin nucleator Arp2/3 complex localizes at the cortex and is essential for actin polymerization during oocyte meiosis (*8, 29*). These results suggested that FMNL2 might be involved in cytokinesis and asymmetric division by regulating actin assembly during mouse oocyte maturation.

The spindle migration is a key step in ensuring the asymmetric division for oocytes (*30*). In mitosis, spindle position is decided by cortical actin and astral microtubules; in contrast, spindle migration is mainly mediated by actin filaments during oocyte meiosis (*30, 31*). Due to the effects of FMNL2 on asymmetric division and cytoplasmic actin, we analyzed the spindle positioning at late MI, we found that the spindle migration was disturbed after FMNL2 depletion, no matter the cytokinesis occurred or not. Several formin proteins are shown to regulate spindle migration during oocytes meiosis. For example, FMN2 nucleates actin surrounding the spindle, pushing force generated by actin to trigger the spindle migration (*19, 22*), and cyclin-dependent kinase 1 (Cdk1) induces cytoplasmic Formin-mediated F-actin polymerization to propel the spindle into the cortex (*32*). Our previous studies also showed that absence of the formin family member FMNL1 or FHOD1 could lead to the decrease of cytoplasmic actin to prevent

the spindle migration (*20, 27*). We speculated that FMNL2 together with other Formin proteins, conservatively regulate actin-mediated spindle migration during oocyte meiosis.

Another important finding is that through the mass spectrometry analysis we found many candidate proteins which were related with ER, and our results indicated that FMNL2 was essential for the maintenance of ER distribution in the cytoplasm. Moreover, the loss of FMNL2 induced ER stress, showing with altered expression of GRP78 and CHOP. Proper distribution of ER is important for the oocyte quality. ER displays a homogeneous distribution pattern throughout the entire ooplasm during development of oocytes and embryos from diabetic mice(*33*). During the transition of mouse oocytes from MI to MII phase, actin regulates cortical ER aggregation(*34*). In addition, Formin2 is shown to colocalize with the ER during oocyte meiosis and the ER-associated Formin2 at the spindle periphery is required for MI chromosome migration(*6*). In our results we showed that FMNL2 associated with INF2 protein in oocytes. INF2 is an ER-associated protein, and the expression of GFP-INF2 which containing DAD/WH2 mutations causes the ER to collapse around the nucleus (*35*). We concluded that FMNL2 might regulate INF2 for the distribution of ER in cytoplasm of oocytes.

Besides its roles of ER distribution, it is shown that INF2 also affects mitochondrial length and ER-mitochondrial interaction in an actin-dependent manner (*35, 36*). It is shown that INF2 regulates Drp1 for mitochondrial fission, and INF2-induced actin filaments may drive initial mitochondrial constriction, which allows

Drp1-driven secondary constriction(*36, 37*). In addition, we also found many candidate proteins which were related with mitochondria from mass spectrometry analysis. During oocyte meiosis, mitochondria gradually accumulated around the spindle after GVBD, and the spindle-peripheral FMN2 and its actin nucleation activity are important for the accumulation of mitochondria in this region (*19*). Our results found that FMNL2 depletion caused agglutination of mitochondria and altered MMP level in the cytoplasm, indicating its roles on the mitochondria distribution and functions. Another formin protein mDia1 is shown to be necessary to induce the anchoring of mitochondria along the cytoskeletal in mammalian CV-1 cells and Drosophila BG2-C2 neuronal cells(*38*). Moreover, the formin interaction protein Spire1C binds INF2 to promote actin assembly on mitochondrial surfaces, and Spire1C disruption could reduce mitochondrial constriction and division(*39*). In addition, our result indicated that cofilin expression decreased in FMNL2 depletion oocytes. Cofilin is an actin-depolymerizing factor and its localization at the mitochondrial fission site is crucial for inducing mitochondrial fission and mitophagy (*40*). Depleting of cofilin resulted in abnormal interconnection and elongation of mitochondria (*41*). Together with its roles on ER, these data indicated that FMNL2 might associate with INF2 and cofilin for the actin-based organelle distribution during oocyte meiosis.

Collectively, we provide a body of evidence showing that FMNL2 associates with Formin2 and Arp2/3 complex for actin assembly, which further regulates spindle migration and INF2/Cofilin-related organelle dynamics during mouse oocyte maturation.

Data Availability

All data generated or analyzed during this study are included in this published article

Acknowledgement

We are particularly grateful to Xiao-Yan Fan and Xing-Hua Wang from Fertility Preservation Laboratory, Reproductive Medicine Center, Guangdong Second Provincial General Hospital for their technical assistance of live cell imaging system.

Contributions

MHP and SCS designed the study. MHP performed the majority of the experiments. SML, ZNP, MHS, XHL, JQJ, YZ contributed to the regents and materials. MHP, XHO and SCS analyzed the data. MHP and SCS wrote the manuscript.

Competing interests

There is no conflict of interest to declare.

Ethics approval and consent to participate

Not applicable.

Consent for publication

Not applicable.

References

1. K. Yi, B. Rubinstein, R. Li, Symmetry breaking and polarity establishment during mouse oocyte maturation. *Philosophical transactions of the Royal Society of London. Series B, Biological sciences* **368**, 20130002 (2013).

2. B. Pan, J. Li, The art of oocyte meiotic arrest regulation. *Reproductive biology and endocrinology : RB&E* **17**, 8 (2019).
3. Q. Y. Sun, H. Schatten, Regulation of dynamic events by microfilaments during oocyte maturation and fertilization. *Reproduction* **131**, 193-205 (2006).
4. S. C. Sun, N. H. Kim, Molecular mechanisms of asymmetric division in oocytes. *Microscopy and microanalysis : the official journal of Microscopy Society of America, Microbeam Analysis Society, Microscopical Society of Canada* **19**, 883-897 (2013).
5. X. Duan, S. C. Sun, Actin cytoskeleton dynamics in mammalian oocyte meiosis. *Biol Reprod* **100**, 15-24 (2019).
6. K. Yi, B. Rubinstein, J. R. Unruh, F. Guo, B. D. Slaughter, R. Li, Sequential actin-based pushing forces drive meiosis I chromosome migration and symmetry breaking in oocytes. *The Journal of cell biology* **200**, 567-576 (2013).
7. H. Li, F. Guo, B. Rubinstein, R. Li, Actin-driven chromosomal motility leads to symmetry breaking in mammalian meiotic oocytes. *Nature cell biology* **10**, 1301-1308 (2008).
8. S. C. Sun, Z. B. Wang, Y. N. Xu, S. E. Lee, X. S. Cui, N. H. Kim, Arp2/3 complex regulates asymmetric division and cytokinesis in mouse oocytes. *PloS one* **6**, e18392 (2011).
9. S. Pfender, V. Kuznetsov, S. Pleiser, E. Kerkhoff, M. Schuh, Spire-type actin nucleators cooperate with Formin-2 to drive asymmetric oocyte division. *Current biology : CB* **21**, 955-960 (2011).
10. S. Kuhn, M. Geyer, Formins as effector proteins of Rho GTPases. *Small GTPases* **5**, e29513 (2014).
11. M. Katoh, M. Katoh, Identification and characterization of human FMNL1, FMNL2 and FMNL3 genes in silico. *International journal of oncology* **22**, 1161-1168 (2003).
12. M. Gardberg, K. Talvinen, K. Kaipio, K. Iljin, C. Kampf, M. Uhlen, O. Carpen, Characterization of Diaphanous-related formin FMNL2 in human tissues. *BMC cell biology* **11**, 55 (2010).
13. F. Kage, M. Winterhoff, V. Dimchev, J. Mueller, T. Thalheim, A. Freise, S. Bruhmann, J. Kollasser, J. Block, G. Dimchev, M. Geyer, H. J. Schnittler, C. Brakebusch, T. E. Stradal, M. F. Carlier, M. Sixt, J. Kas, J. Faix, K. Rottner, FMNL formins boost lamellipodial force generation. *Nature communications* **8**, 14832 (2017).
14. X. L. Zhu, Y. F. Zeng, J. Guan, Y. F. Li, Y. J. Deng, X. W. Bian, Y. Q. Ding, L. Liang, FMNL2 is a positive regulator of cell motility and metastasis in colorectal carcinoma. *The Journal of pathology* **224**, 377-388 (2011).
15. J. Block, D. Breitsprecher, S. Kuhn, M. Winterhoff, F. Kage, R. Geffers, P. Duwe, J. L. Rohn, B. Baum, C. Brakebusch, M. Geyer, T. E. Stradal, J. Faix, K. Rottner, FMNL2 drives actin-based protrusion and migration downstream of Cdc42. *Current biology : CB* **22**, 1005-1012 (2012).
16. Y. Li, X. Zhu, Y. Zeng, J. Wang, X. Zhang, Y. Q. Ding, L. Liang, FMNL2 enhances invasion of colorectal carcinoma by inducing epithelial-mesenchymal transition. *Molecular cancer research : MCR* **8**, 1579-1590 (2010).
17. F. Kage, A. Steffen, A. Ellinger, C. Ranftler, C. Gehre, C. Brakebusch, M. Pavelka, T. Stradal, K. Rottner, Author Correction: FMNL2 and -3 regulate Golgi architecture and anterograde transport downstream of Cdc42. *Scientific reports* **9**, 18008 (2019).
18. D. Breitsprecher, B. L. Goode, Formins at a glance. *Journal of cell science* **126**, 1-7

(2013).

19. X. Duan, Y. Li, K. Yi, F. Guo, H. Wang, P. H. Wu, J. Yang, D. B. Mair, E. A. Morales, P. Kalab, D. Wirtz, S. X. Sun, R. Li, Dynamic organelle distribution initiates actin-based spindle migration in mouse oocytes. *Nature communications* **11**, 277 (2020).
20. F. Wang, L. Zhang, X. Duan, G. L. Zhang, Z. B. Wang, Q. Wang, B. Xiong, S. C. Sun, RhoA-mediated FMNL1 regulates GM130 for actin assembly and phosphorylates MAPK for spindle formation in mouse oocyte meiosis. *Cell cycle* **14**, 2835-2843 (2015).
21. K. Yi, J. R. Unruh, M. Deng, B. D. Slaughter, B. Rubinstein, R. Li, Dynamic maintenance of asymmetric meiotic spindle position through Arp2/3-complex-driven cytoplasmic streaming in mouse oocytes. *Nature cell biology* **13**, 1252-1258 (2011).
22. J. Dumont, K. Million, K. Sunderland, P. Rassinier, H. Lim, B. Leader, M. H. Verlhac, Formin-2 is required for spindle migration and for the late steps of cytokinesis in mouse oocytes. *Developmental biology* **301**, 254-265 (2007).
23. B. Leader, H. Lim, M. J. Carabatsos, A. Harrington, J. Ecsedy, D. Pellman, R. Maas, P. Leder, Formin-2, polyploidy, hypofertility and positioning of the meiotic spindle in mouse oocytes. *Nature cell biology* **4**, 921-928 (2002).
24. K. Grikscheit, T. Frank, Y. Wang, R. Grosse, Junctional actin assembly is mediated by Formin-like 2 downstream of Rac1. *The Journal of cell biology* **209**, 367-376 (2015).
25. X. L. Ren, Y. D. Qiao, J. Y. Li, X. M. Li, D. Zhang, X. J. Zhang, X. H. Zhu, W. J. Zhou, J. Shi, W. Wang, W. T. Liao, Y. Q. Ding, L. Liang, Cortactin recruits FMNL2 to promote actin polymerization and endosome motility in invadopodia formation. *Cancer letters* **419**, 245-256 (2018).
26. Y. Lu, Y. Zhang, M. H. Pan, N. H. Kim, S. C. Sun, X. S. Cui, Daam1 regulates fascin for actin assembly in mouse oocyte meiosis. *Cell cycle* **16**, 1350-1356 (2017).
27. M. H. Pan, F. Wang, Y. Lu, F. Tang, X. Duan, Y. Zhang, B. Xiong, S. C. Sun, FHOD1 regulates cytoplasmic actin-based spindle migration for mouse oocyte asymmetric cell division. *Journal of cellular physiology* **233**, 2270-2278 (2018).
28. Y. Zhang, F. Wang, Y. J. Niu, H. L. Liu, R. Rui, X. S. Cui, N. H. Kim, S. C. Sun, Formin mDia1, a downstream molecule of FMNL1, regulates Profilin1 for actin assembly and spindle organization during mouse oocyte meiosis. *Biochimica et biophysica acta* **1853**, 317-327 (2015).
29. E. D. Goley, M. D. Welch, The ARP2/3 complex: an actin nucleator comes of age. *Nature reviews. Molecular cell biology* **7**, 713-726 (2006).
30. S. Brunet, B. Maro, Cytoskeleton and cell cycle control during meiotic maturation of the mouse oocyte: integrating time and space. *Reproduction* **130**, 801-811 (2005).
31. S. Reinsch, P. Gonczy, Mechanisms of nuclear positioning. *Journal of cell science* **111 (Pt 16)**, 2283-2295 (1998).
32. Z. Wei, J. Greaney, C. Zhou, A. H. H, Cdk1 inactivation induces post-anaphase-onset spindle migration and membrane protrusion required for extreme asymmetry in mouse oocytes. *Nature communications* **9**, 4029 (2018).
33. C. H. Zhang, W. P. Qian, S. T. Qi, Z. J. Ge, L. J. Min, X. L. Zhu, X. Huang, J. P. Liu, Y. C. Ouyang, Y. Hou, H. Schatten, Q. Y. Sun, Maternal diabetes causes abnormal dynamic changes of endoplasmic reticulum during mouse oocyte maturation and early embryo development. *Reproductive biology and endocrinology : RB&E* **11**, 31 (2013).

34. G. FitzHarris, P. Marangos, J. Carroll, Changes in endoplasmic reticulum structure during mouse oocyte maturation are controlled by the cytoskeleton and cytoplasmic dynein. *Dev Biol* **305**, 133-144 (2007).
35. E. S. Chhabra, V. Ramabhadran, S. A. Gerber, H. N. Higgs, INF2 is an endoplasmic reticulum-associated formin protein. *Journal of cell science* **122**, 1430-1440 (2009).
36. F. Korobova, V. Ramabhadran, H. N. Higgs, An actin-dependent step in mitochondrial fission mediated by the ER-associated formin INF2. *Science* **339**, 464-467 (2013).
37. W. K. Ji, R. Chakrabarti, X. Fan, L. Schoenfeld, S. Strack, H. N. Higgs, Receptor-mediated Drp1 oligomerization on endoplasmic reticulum. *The Journal of cell biology* **216**, 4123-4139 (2017).
38. A. A. Minin, A. V. Kulik, F. K. Gyoeva, Y. Li, G. Goshima, V. I. Gelfand, Regulation of mitochondria distribution by RhoA and formins. *Journal of cell science* **119**, 659-670 (2006).
39. U. Manor, S. Bartholomew, G. Golani, E. Christenson, M. Kozlov, H. Higgs, J. Spudich, J. Lippincott-Schwartz, A mitochondria-anchored isoform of the actin-nucleating spire protein regulates mitochondrial division. *eLife* **4**, (2015).
40. G. B. Li, H. W. Zhang, R. Q. Fu, X. Y. Hu, L. Liu, Y. N. Li, Y. X. Liu, X. Liu, J. J. Hu, Q. Deng, Q. S. Luo, R. Zhang, N. Gao, Mitochondrial fission and mitophagy depend on cofilin-mediated actin depolymerization activity at the mitochondrial fission site. *Oncogene* **37**, 1485-1502 (2018).
41. S. Li, S. Xu, B. A. Roelofs, L. Boyman, W. J. Lederer, H. Sesaki, M. Karbowski, Transient assembly of F-actin on the outer mitochondrial membrane contributes to mitochondrial fission. *The Journal of cell biology* **208**, 109-123 (2015).

Figure legends

Figure 1. Expression and subcellular localization of FMNL2 during mouse oocyte meiosis. (A) Western blotting results of FMNL2 protein expression at different stages. FMNL2 expressed at the GV, MI, and MII stages. **(B)** Subcellular localization of FMNL2-EGFP during mouse oocyte meiosis. FMNL2 was enriched at the cortex (GV, GVBD and MI stage) and spindle periphery (MI stage). Green, FMNL2-EGFP; blue, DNA. Negative control: Green, EGFP; blue, DNA. Bar =20 μm. **(C)** Co-staining of oocytes for FMNL2 and actin. FMNL2 and actin overlapped in cortex and spindle surrounding. Green, FMNL2-antibody; red, actin; blue, DNA. Bar =20 μm.

Figure 2. Knockdown of FMNL2 affects first polar body extrusion and asymmetric

566 **division. (A)** Western blot analysis for FMNL2 expression in the FMNL2-KD group
567 and control group. Relative intensity of FMNL2 and tubulin was assessed by
568 densitometry. **, significant difference ($P < 0.01$). **(B)** DIC images of control oocytes
569 and FMNL2-KD oocytes after 12 h culture. FMNL2-KD caused large polar bodies
570 (black arrows) and some oocytes failed to extrude the polar bodies (white arrows). (**C**)
571 Rate of polar body extrusion after 12 h culture of the control group and FMNL2-KD
572 group. ***, significant difference ($P < 0.001$). **(D)** Rate of large polar body extrusion
573 after 12 h culture in the control group and FMNL2-KD group. ****, significant
574 difference ($P < 0.0001$). **(E)** Time-lapse microscopy showed that polar body extrusion
575 failed after FMNL2-KD. Bar = 10 μm. **(F)** Western blot analysis for FMNL2 expression
576 in the control group, FMNL2-KD group and rescue group. Relative intensity of FMNL2
577 and tubulin was assessed by densitometry. **(G)** DIC images of FMNL2-KD oocytes and
578 rescue oocytes after 12 h culture. (**H)** Rate of polar body extrusion after 12 h culture of
579 the FMNL2-KD group and rescue group. *, significant difference ($P < 0.05$). **(I)** Rate
580 of large polar body extrusion after 12 h culture in the FMNL2-KD group and rescue
581 group. ***, significant difference ($P < 0.001$). (**J)** Rate of polar body extrusion after 12
582 h culture of the control group and FMNL2+3-KD group. *, significant difference ($P <$
583 0.05). **(K)** Rate of large polar body extrusion after 12 h culture in the control group and
584 FMNL2+3-KD group. ***, significant difference ($P < 0.001$).

585 **Figure 3. Knockdown of FMNL2 disrupts spindle localization during mouse**
586 **oocyte meiosis. (A)** Time-lapse microscopy showed that spindle migration failed after
587 FMNL2-KD. Green, tubulin-EGFP. Bar = 10 μm. **(B)** Representative images and the

proportion of spindle migration after 9.5 h of culture in the control group and FMNL2-KD oocyte group. White, actin; green, tubulin; magenta, DNA. Bar = 10 μm. *, significant difference ($P < 0.05$). **(C)** Representative images and the proportion of spindle migration after 9.5 h of culture in the FMNL2-KD group and rescue oocyte group. magenta, DNA. Bar = 10 μm. *, significant difference ($P < 0.01$).

Figure 4. Knockdown of FMNL2 disrupts actin assembly during mouse oocyte meiosis. (A) Representative images of actin distribution at the oocyte cortex and the fluorescent intensities in the control group and FMNL2-KD group ($P > 0.1$). White, actin; green, tubulin; magenta, DNA. Bar = 10 μm. **(B)** Representative images of actin distribution in the oocyte cytoplasm and the fluorescent intensities in the control group and FMNL2-KD group. White, actin; green, tubulin; magenta, DNA. Bar = 10 μm. ****, significant difference ($P < 0.0001$). **(C)** Representative images of actin distribution in the oocyte cytoplasm and the fluorescent intensities in the FMNL2-KD group and rescue group. White, actin; magenta, DNA. Bar = 10 μm. ****, significant difference ($P < 0.0001$) **(D)** Mass spectrometry results showed that FMNL2 was related to many actin-related proteins. **(E)** Co-IP results showed that FMNL2 was correlated with Arp and Formin2 but not with Profiling and Fascin. **(F)** Arp2 protein expression significantly increased in the FMNL2-KD oocytes compared with the control oocytes. Arp2 protein expression significantly decreased in the rescue oocytes compared with the FMNL2-KD oocytes. **, significant difference ($P < 0.01$). **(G)** Formin2 protein expression significantly decreased in the FMNL2-KD oocytes compared with the control oocytes. Formin2 protein expression significantly increased in the rescue

oocytes compared with the FMNL2-KD oocytes. **, significant difference ($P < 0.01$).

Figure 5. FMNL2 regulates endoplasmic reticulum distribution during mouse oocytes maturation. (A) Co-IP results showed that FMNL2 was correlated with INF2. **(B)** Mass spectrometry results showed that FMNL2 was associated with ER-related proteins. **(C)** Representative images of ER distribution in the oocyte cytoplasm in the control group and FMNL2-KD group. In FMNL2-KD oocytes, ER agglomerated in cytoplasm (white arrow). Red, ER; Blue, DNA. Bar = 10 μm. **(D)** Abnormal distribution of ER significantly increased in the FMNL2-KD oocytes compared with the control oocytes. *, significant difference ($P < 0.05$). **(E)** Grp78 and Chop protein expression significantly increased in the FMNL2-KD oocytes compared with the control oocytes. The band intensity analysis also confirmed this finding. *, significant difference ($P < 0.05$). **(F)** Representative images of ER distribution in the oocyte cytoplasm in the FMNL2-KD group and rescue group. Red, ER; Blue, DNA. Bar = 10 μm. **(G)** Abnormal distribution of ER significantly decreased in the rescue oocytes compared with the FMNL2-KD oocytes. *, significant difference ($P < 0.05$). **(H)** Grp78 protein expression significantly decreased in the rescue oocytes compared with the FMNL2-KD oocytes. The band intensity analysis also confirmed this finding. **, significant difference ($P < 0.01$).

Figure 6. FMNL2 regulates mitochondrial distribution during mouse oocytes maturation. (A) Mass spectrometry results showed that FMNL2 was related to many mitochondria-related proteins. **(B)** Representative images of mitochondrial distribution in the oocyte cytoplasm in the control group and FMNL2-KD group. In FMNL2-KD

oocytes, mitochondrial agglomerated in cytoplasm (white arrow). Green, Mito. Bar = 20 μm. **(C)** Abnormal distribution of mitochondrial significantly increased in the FMNL2-KD oocytes compared with the control oocytes. *, significant difference ($P < 0.05$). **(D)** Representative images of mitochondrial distribution in the oocyte cytoplasm in the FMNL2-KD group and rescue group. In FMNL2-KD oocytes, mitochondrial agglomerated in cytoplasm (white arrow). Red, Mito; Blue, DNA. Bar = 20 μm. **(E)** Abnormal distribution of mitochondrial significantly decreased in the rescue oocytes compared with the FMNL2-KD oocytes. **, significant difference ($P < 0.01$). **(F)** The typical picture for JC1 green channel and red channel after FMNL2-KD. **(G)** The JC1 signal (red/green ratio) after FMNL2-KD compare with the control group, the JC-1 red/green fluorescence ratio was significantly reduced in FMNL2-KD groups. Bar = 20 μm. **, $P < 0.01$. **(H)** cofilin protein expression significantly decreased in the FMNL2-KD oocytes compared with the control oocytes. The band intensity analysis also confirmed this finding. *, significant difference ($P < 0.05$).

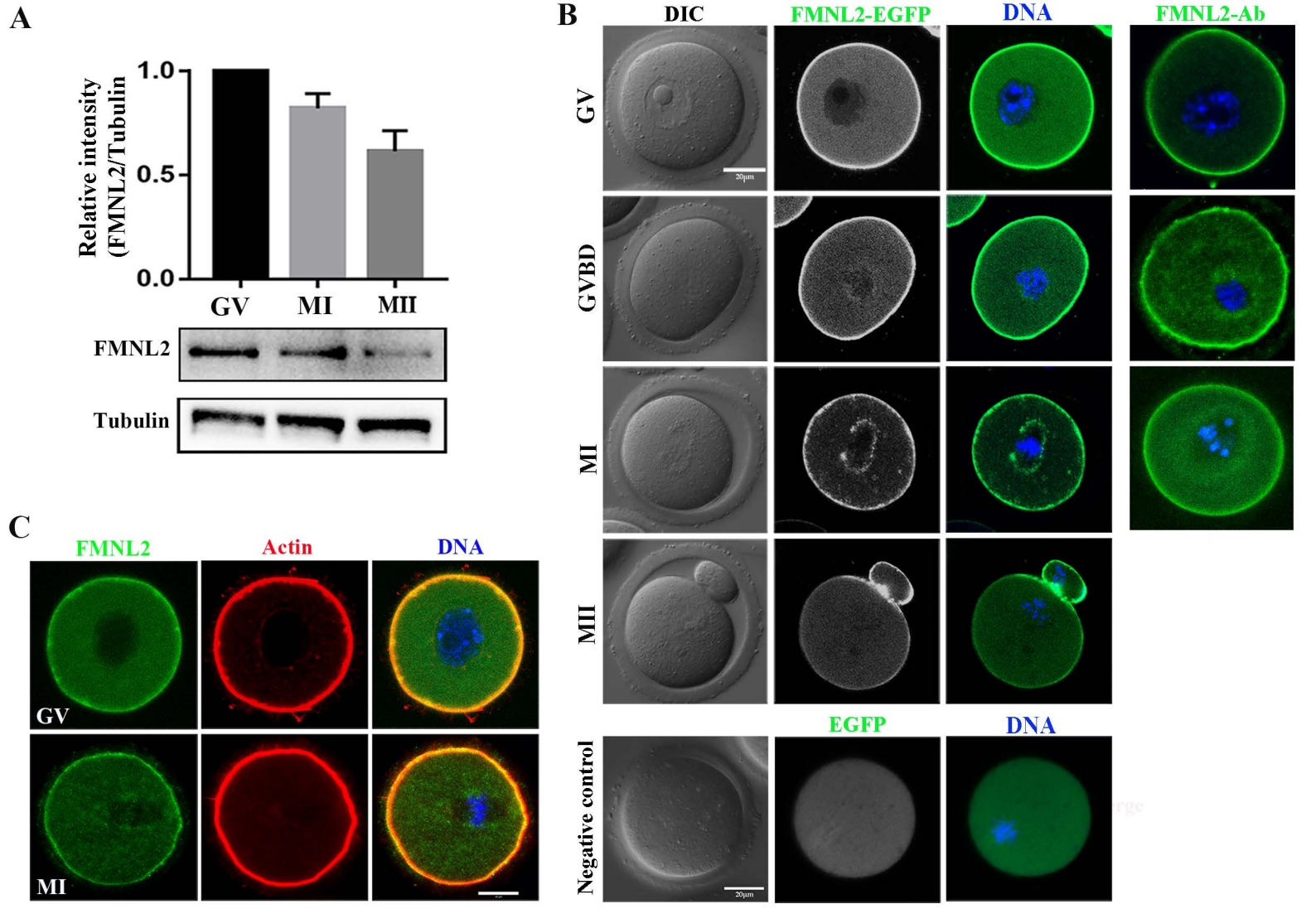
A
Relative intensity (FMNL2/Tubulin
1.0
0.5
0.0
GV
MI
MII
FMNL2
Tubulin
B
DIC
FMNL2-EGFP
DNA
FMNL2-Ab
GV
GVBD
MI
MII
EGFP
DNA
Negative control
C
FMNL2
Actin
DNA
GV
MI

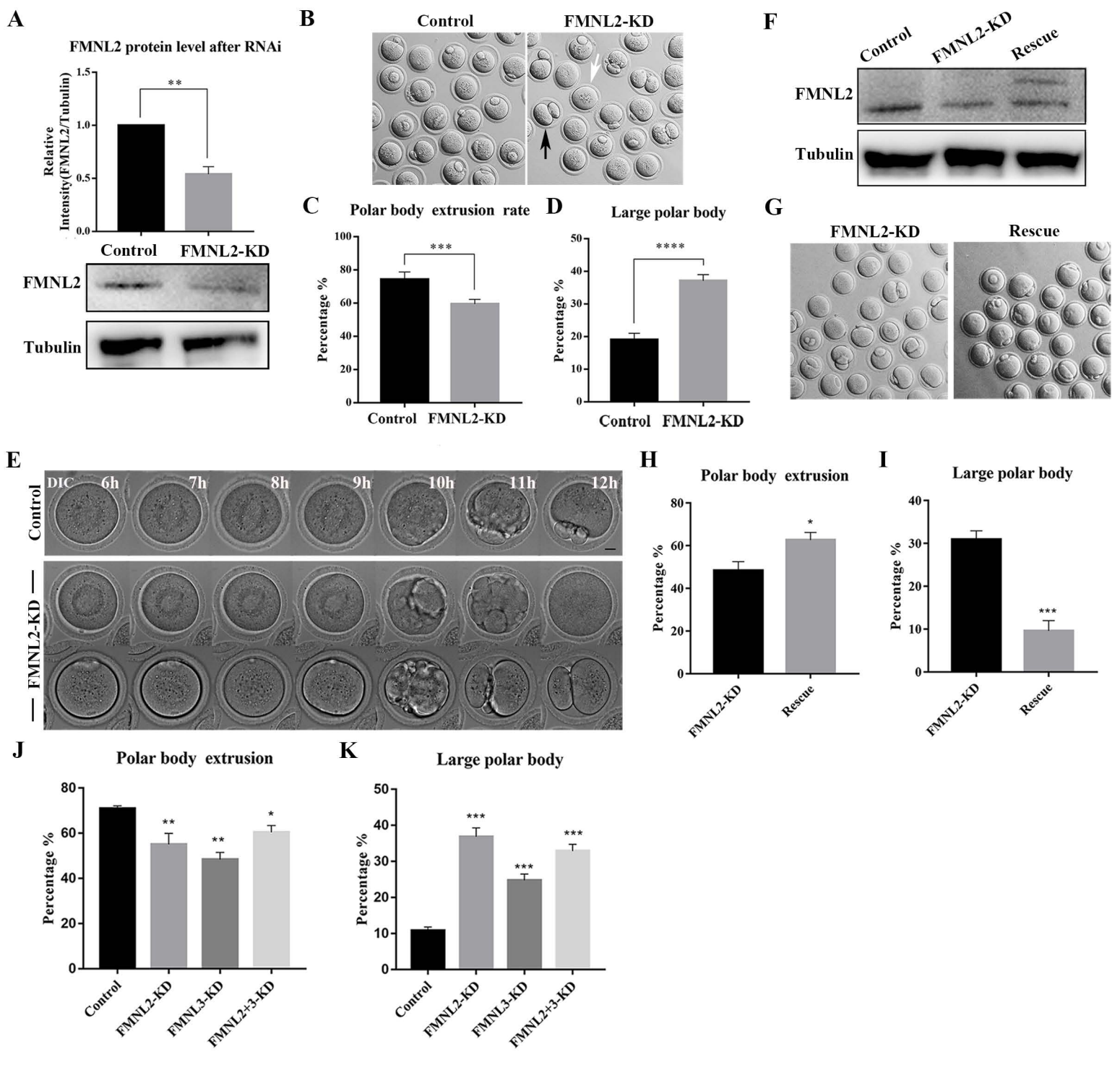
A
FMNL2 protein level after RNAi
Relative Intensity(FMNL2/Tubulin)
1.5
1.0
0.5
0.0
**
Control
FMNL2-KD
FMNL2
Tubulin
B
Control
FMNL2-KD
C
Polar body extrusion rate
Percentage %
100
80
60
40
20
0
***
Control
FMNL2-KD
D
Large polar body
Percentage %
50
40
30
20
10
0
****
Control
FMNL2-KD
F
Control
FMNL2-KD
Rescue
FMNL2
Tubulin
G
FMNL2-KD
Rescue
E
DIC
6h
7h
8h
9h
10h
11h
12h
Control
FMNL2-KD
H
Polar body extrusion
Percentage %
80
60
40
20
0
*
FMNL2-KD
Rescue
I
Large polar body
Percentage %
40
30
20
10
0
***
FMNL2-KD
Rescue
J
Polar body extrusion
Percentage %
80
60
40
20
0
**
**
*
Control
FMNL2-KD
FMNL3-KD
FMNL2+3-KD
K
Large polar body
Percentage %
50
40
30
20
10
0
***
***
***
Control
FMNL2-KD
FMNL3-KD
FMNL2+3-KD

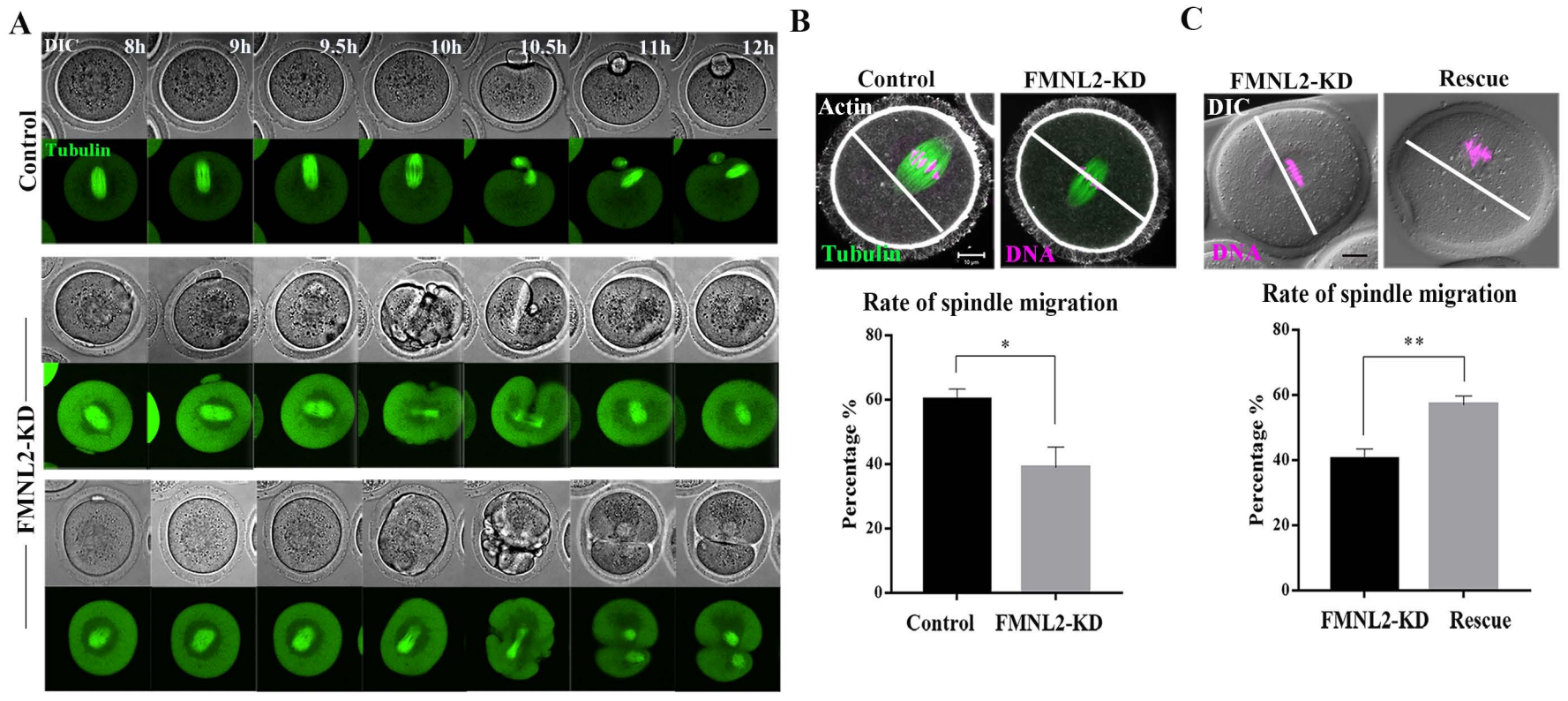
A
DIC
8h
9h
9.5h
10h
10.5h
11h
12h
Control
Tubulin
FMNL2-KD
B
Control
FMNL2-KD
Actin
Tubulin
DNA
Rate of spindle migration
Percentage %
80
60
40
20
0
*
Control
FMNL2-KD
C
FMNL2-KD
Rescue
DIC
DNA
Rate of spindle migration
Percentage %
80
60
40
20
0
**
FMNL2-KD
Rescue

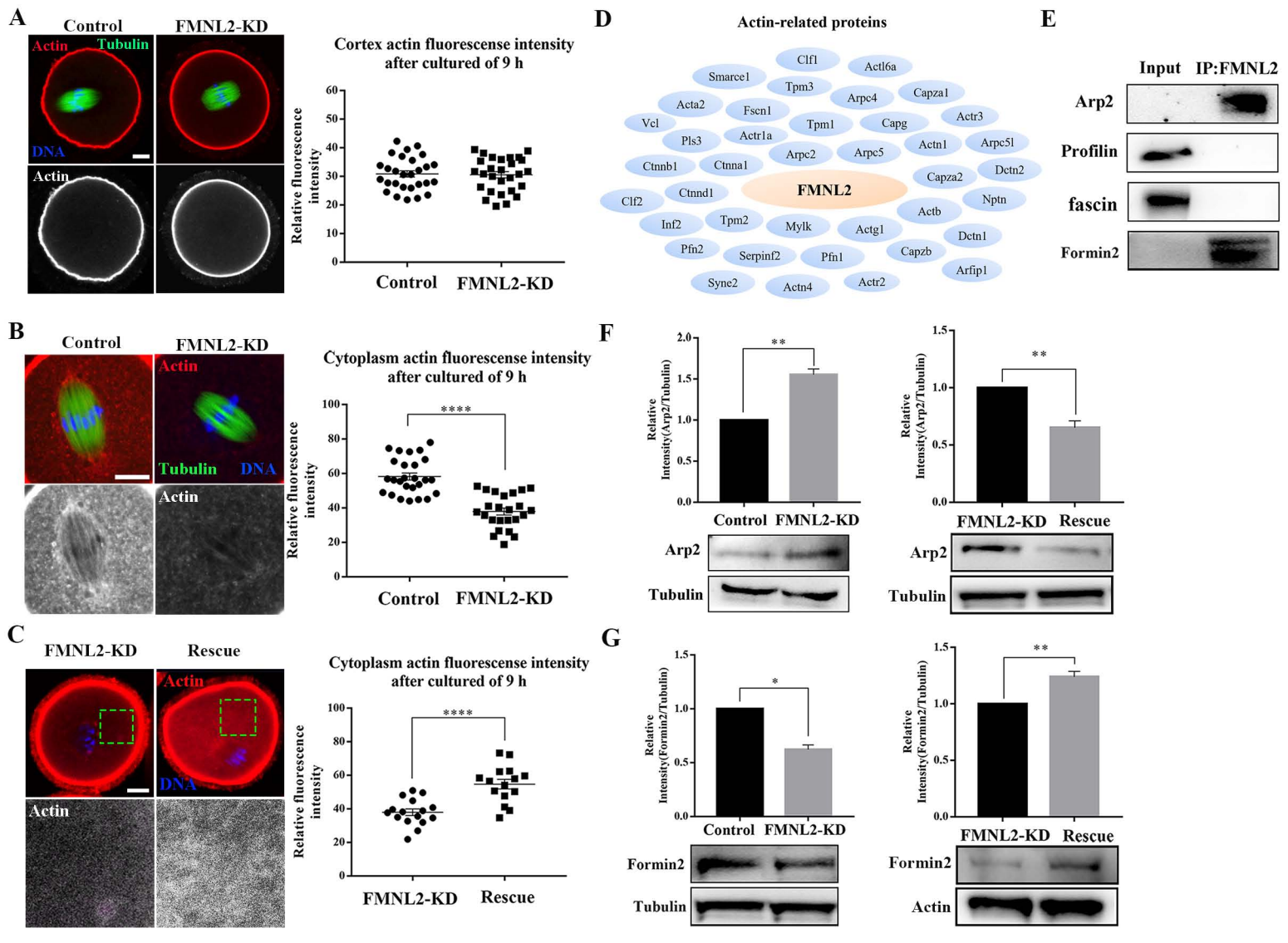
A
Control
FMNL2-KD
Actin
Tubulin
DNA
Actin
Cortex actin fluorescense intensity after cultured of 9 h
Relative fluorescence intensity
Control
FMNL2-KD
B
Control
FMNL2-KD
Actin
Tubulin
DNA
Actin
Cytoplasm actin fluorescense intensity after cultured of 9 h
****
Relative fluorescence intensity
Control
FMNL2-KD
C
FMNL2-KD
Rescue
Actin
DNA
Actin
Cytoplasm actin fluorescense intensity after cultured of 9 h
****
Relative fluorescence intensity
FMNL2-KD
Rescue
D
Actin-related proteins
Clf1
Actl6a
Smarce1
Tpm3
Arpc4
Capza1
Acta2
Fscn1
Actr3
Vcl
Tpm1
Capg
Pls3
Actr1a
Arpc5l
Actn1
Arpc2
Arpc5
Ctnnb1
Ctnna1
Capza2
Dctn2
Clf2
Ctnnd1
FMNL2
Nptn
Actb
Inf2
Tpm2
Mylk
Actg1
Dctn1
Pfn2
Serpinf2
Pfn1
Capzb
Arfip1
Syne2
Actn4
Actr2
E
Input
IP:FMNL2
Arp2
Profilin
fascin
Formin2
F
**
Relative Intensity(Arp2/Tubulin)
Control
FMNL2-KD
Arp2
Tubulin
**
Relative Intensity(Arp2/Tubulin)
FMNL2-KD
Rescue
Arp2
Tubulin
G
*
Relative Intensity(Formin2/Tubulin)
Control
FMNL2-KD
Formin2
Tubulin
**
Relative Intensity(Formin2/Tubulin)
FMNL2-KD
Rescue
Formin2
Actin

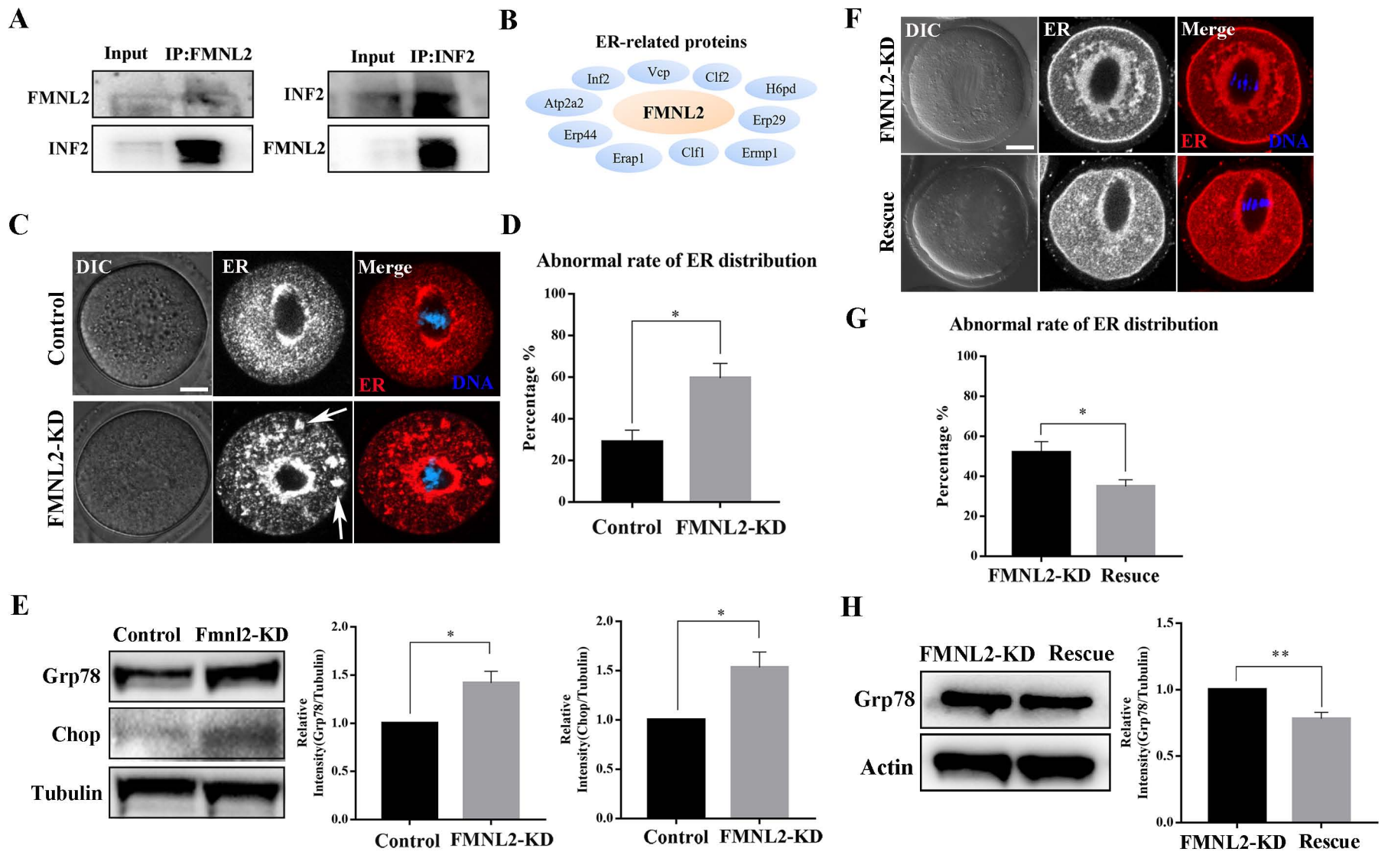
A
Input IP:FMNL2
FMNL2
INF2
Input IP:INF2
INF2
FMNL2
B
ER-related proteins
Inf2
Vcp
Clf2
H6pd
Atp2a2
FMNL2
Erp29
Erp44
Erap1
Clf1
Ermp1
C
DIC
ER
Merge
Control
FMNL2-KD
ER
DNA
D
Abnormal rate of ER distribution
Percentage %
100
80
60
40
20
0
*
Control FMNL2-KD
F
DIC
ER
Merge
FMNL2-KD
Rescue
ER
DNA
G
Abnormal rate of ER distribution
Percentage %
100
80
60
40
20
0
*
FMNL2-KD Resuce
E
Control Fmnl2-KD
Grp78
Chop
Tubulin
Relative Intensity(Grp78/Tubulin)
2.0
1.5
1.0
0.5
0.0
*
Control FMNL2-KD
Relative Intensity(Chop/Tubulin)
2.0
1.5
1.0
0.5
0.0
*
Control FMNL2-KD
H
FMNL2-KD Rescue
Grp78
Actin
Relative Intensity(Grp78/Tubulin)
1.5
1.0
0.5
0.0
**
FMNL2-KD Rescue

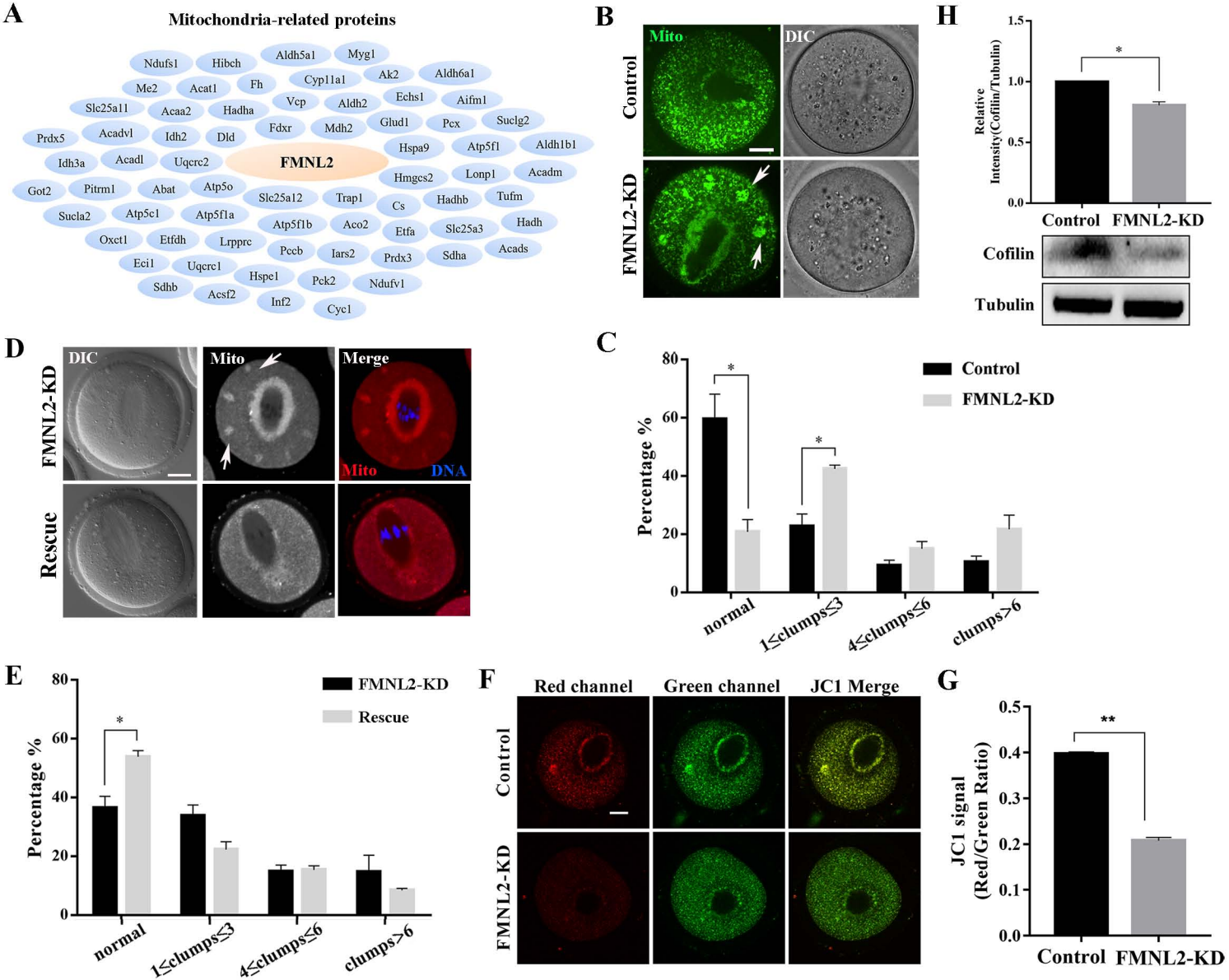
A
Mitochondria-related proteins
Ndufs1
Hibch
Aldh5a1
Myg1
Me2
Acat1
Fh
Cyp11a1
Ak2
Aldh6a1
Slc25a11
Acaa2
Hadha
Vcp
Aldh2
Echs1
Aifm1
Prdx5
Acadvl
Idh2
Dld
Fdxr
Mdh2
Glud1
Pcx
Suclg2
Idh3a
Acadl
Uqcrc2
FMNL2
Hspa9
Atp5f1
Aldh1b1
Got2
Pitrm1
Abat
Atp5o
Hmgcs2
Lonp1
Acadm
Sucla2
Atp5c1
Atp5f1a
Slc25a12
Trap1
Cs
Hadhb
Tufm
Oxct1
Etfdh
Lrpprc
Atp5f1b
Aco2
Etfa
Slc25a3
Hadh
Eci1
Uqcrc1
Pccb
Iars2
Prdx3
Sdha
Acads
Sdhb
Acsf2
Hspe1
Inf2
Pck2
Cyc1
Ndufv1
B
Control
FMNL2-KD
Mito
DIC
H
Relative Intensity(Cofilin/Tubulin)
1.5
1.0
0.5
0.0
*
Control
FMNL2-KD
Cofilin
Tubulin
D
FMNL2-KD
Rescue
DIC
Mito
Merge
Mito
DNA
C
Percentage %
80
60
40
20
0
*
*
Control
FMNL2-KD
normal
1≤clumps≤3
4≤clumps≤6
clumps>6
E
Percentage %
80
60
40
20
0
*
FMNL2-KD
Rescue
normal
1≤clumps≤3
4≤clumps≤6
clumps>6
F
Red channel
Green channel
JC1 Merge
Control
FMNL2-KD
G
JC1 signal (Red/Green Ratio)
0.5
0.4
0.3
0.2
0.1
0.0
**
Control
FMNL2-KD